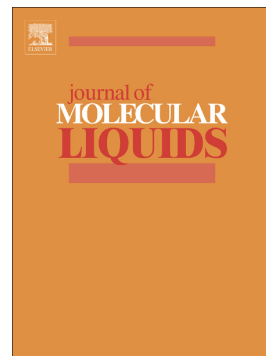


Journal Pre-proof

A novel dual-function probe for recognition and differentiation of Zn²⁺ and Al³⁺ and its application

Ting-Ting Liu, Jiao Xu, Cheng-guo Liu, Shuang Zeng, Zhi-Yong Xing, Xue-Jiao Sun, Jin-Long Li



PII: S0167-7322(19)35166-9

DOI: <https://doi.org/10.1016/j.molliq.2019.112250>

Reference: MOLLIQ 112250

To appear in: *Journal of Molecular Liquids*

Received date: 14 September 2019

Revised date: 27 November 2019

Accepted date: 30 November 2019

Please cite this article as: T.-T. Liu, J. Xu, C.-g. Liu, et al., A novel dual-function probe for recognition and differentiation of Zn²⁺ and Al³⁺ and its application, *Journal of Molecular Liquids*(2018), <https://doi.org/10.1016/j.molliq.2019.112250>

This is a PDF file of an article that has undergone enhancements after acceptance, such as the addition of a cover page and metadata, and formatting for readability, but it is not yet the definitive version of record. This version will undergo additional copyediting, typesetting and review before it is published in its final form, but we are providing this version to give early visibility of the article. Please note that, during the production process, errors may be discovered which could affect the content, and all legal disclaimers that apply to the journal pertain.

© 2018 Published by Elsevier.

A novel dual-function probe for recognition and differentiation of Zn^{2+} and Al^{3+} and its application

Ting-Ting Liu ^{a,1}, Jiao Xu ^{b,1}, Cheng-guo Liu ^a, Shuang Zeng ^a, Zhi-Yong Xing ^{a,*}, Xue-Jiao Sun ^a,

Jin-Long Li ^{c,*}

^a Department of Applied Chemistry, College of Science, Northeast Agricultural University, Harbin 150030, PR China.

^b Jiamusi College, Heilongjiang University of Chinese Medicine, Harbin, China.

^c School of Chemistry and Chemical Engineering, Qiqihar University, Qiqihar 161006, PR China.

* Corresponding authors

E-mail addresses: zyxing@neau.edu.cn; jinlong141@163.com

¹ These authors contributed equally to this work.

Abstract: A dual-function probe **BHMH** was synthesized and characterized functioned with benzothiazole as signal unit for the simultaneous detection of Zn^{2+} and Al^{3+} DMF/H₂O (1/1, v/v, 0.01M HEPES, pH = 6.0). Probe **BHMH** achieved in the recognition of Zn^{2+} and Al^{3+} both through obvious fluorescence turn-on and absorbance ratiometric response. The limit of detection (LOD) according to the titration of fluorescence for Zn^{2+} and Al^{3+} were 1.27×10^{-7} M and 1.42×10^{-7} M, respectively. Furthermore, the significant color changes could be detected by naked eye whatever under ultraviolet-lamp or daylight. According to Job plot, the binding ratio of **BHMH** with Zn^{2+} and Al^{3+} were determined as 1:1 and 2:1, respectively. The binding detail was further confirmed by ¹H NMR titration and ESI-MS analysis as well. Moreover, probe **BHMH** was successfully applied in the detection Zn^{2+} and Al^{3+} in real sample and test stripe.

Key word: Fluorescence; Dual-function; Al^{3+} ; Zn^{2+}

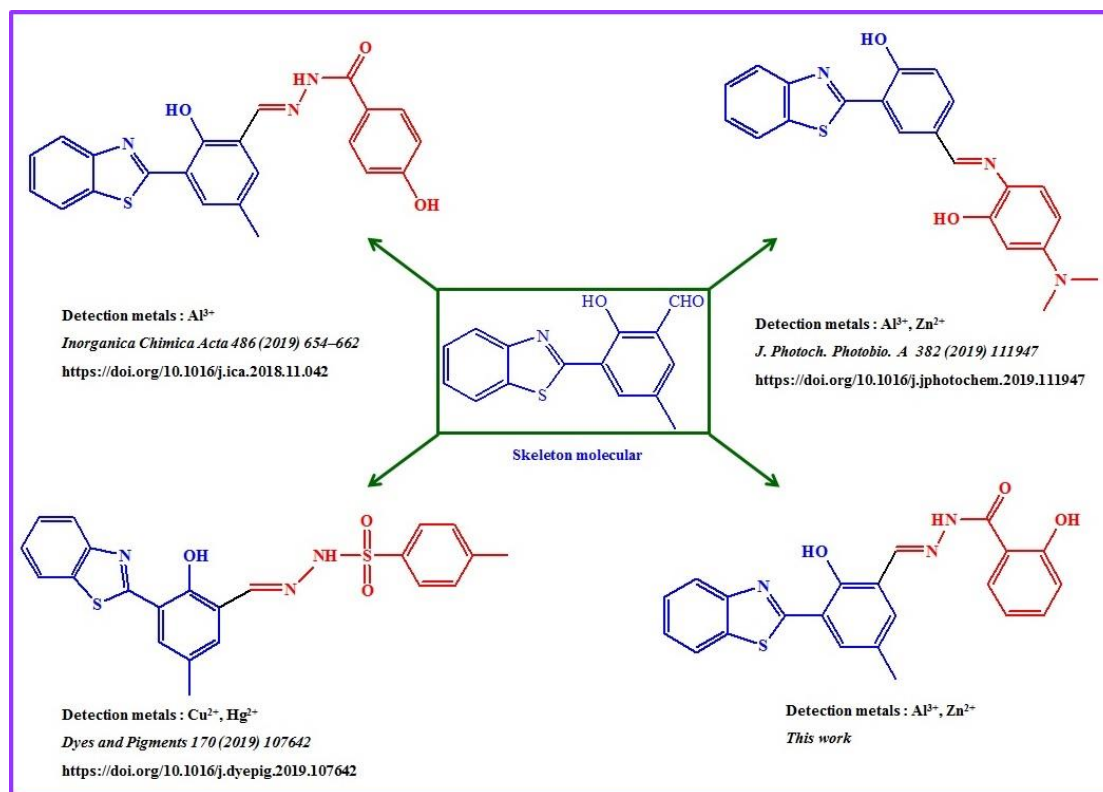
1. Introduction

Aluminum, among the richest elements in earth crust, is closely related to human daily living due to its widely used in many fields (such as package of foods and drugs, kitchen utensils, and water treatment equipment). However, Al^{3+} which is the most existence ionic style of aluminum in water and plant body and the unnecessary element for mankind, is inevitable accumulated in human body through the water and food. However, the upper limitation of daily intake is 10 mg according to the recommendation of World Health Organization (WHO), and over accumulation in body will induce neurodegenerative diseases such as Alzheimer's disease and Parkinson's disease [1-6]. On the contrary, as the second most abundant transition metal and a necessary element for human body, Zinc (Zn), acts as a key role in many functional processes such as signal transmitters, cellular metabolism, and neural immune function. However, whatever insufficient intake or excessive ingestion of Zn^{2+} is detrimental to the health of mankind [7-11]. Hence, it is essential to develop an efficient method of trace detection Al^{3+} and Zn^{2+} for the health of human beings and environmental protection as well.

Up to now, it has been a hot topic for researchers that is in the development of fluorescent probes for the trace detection of various analyte, which mainly due to its unique properties including high sensitivity, real-time response, facile operation and naked-eye detection [12-14]. Up to now, many excellent fluorescence probes were reported for different metal ions based on different mechanism and designing idea. Among them, that one probe for simultaneous multi-target detection, which showed its merits such as high efficiency, time and cost saving, is becoming popular to researchers in the development of fluorescence probes. Lots of multi-functional fluorescence probes for multiple targets simultaneous detection were reported with various

fluorophore [15-55], some of them were Al^{3+} and Zn^{2+} fluorescent probes based on various fluorophore [38-55] such as thiophene [38], diarylethene [39-43], squaraine [44], aza-crown [45], hydrazine [46], chromone-rhodamine [47], acylhydrazone [48], triphenylamine [49], chromen [50], naphthalene [51], alicyldehyde [52], biphenyl-anthracene [53] and benzothiazole [54, 55], but only a few of them were based on benzothiazole fluorophore. Hence, the development of benzothiazole-based fluorescent probe for simultaneous detection of Al^{3+} and Zn^{2+} is still full of charming.

2-(2-hydroxyphenyl)benzothiazole, one of excellent acceptors in D- π -A structures considering its electron withdrawing ability, is widely used as an idea fluorophore in construction fluorescent probe through conjugation with proton donating group such as hydroxyl group, which is characterized as excited state intramolecular proton transfer (ESIPT) mechanism with significant fluorescence signal change and larger Stokes shift as well. Some previous related works (**Scheme 1**) [29, 55, 56] lighted us the idea that the compound synthesized by condensation of the skeleton molecular (3-(benzo[d]thiazol-2-yl)-2-hydroxy-5-methylbenzaldehyde) with 2-hydroxybenzohydrazide might helpful to achieve in the development of dual functional probe for Al^{3+} and Zn^{2+} . Hence, (*E*)-3-(benzo[d]thiazol-2-yl)-2-hydroxy-5-methylbenzaldehyde salicyl acylhydrazone (**BHMH**) was synthesized (**Scheme 2**) and its spectrum performance was systematic investigated. **BHMH** showed highly sensitivity to Al^{3+} and Zn^{2+} manifested in obvious fluorescence turn-on and color change, respectively. Al^{3+} and Zn^{2+} could be differentiated by adding EDTA which is a common reagent be usually used in revisable experiment. Moreover, **BHMH** was achieved in the application in real sample detection of Al^{3+} and Zn^{2+} with high sensitivity and accuracy.



Scheme 1 Designing idea for probe **BMMH**

2. Experimental

2.1 Materials and apparatus

All analytical reagent grade chemicals and solvents employed for the synthesis and characterization were purchased from commercial sources and used as received without any treatment. Nuclear magnetic resonance spectra (NMR) were recorded on a Bruker 600 MHz system, and the chemical shifts are reported in ppm with Me_4Si as the internal standard. High resolution mass spectroscopy (HRMS) was carried out on a Waters Xevo UPLC/G2-SQ ToF MS spectrometer. The FT-IR spectra were recorded on a Bruker ALPHA-T by dispersing samples in KBr disks, in the range of $4000\text{--}400\text{ cm}^{-1}$. The UV–vis absorption and fluorescence spectra of the samples were measured on Pgeneral TU-255 UV-vis Spectrophotometer and Perkin Elmer LS55 fluorescence spectrometer, respectively.

2.2. General information

Stock solutions of the metal ions (Al^{3+} , Fe^{3+} , Cr^{3+} , Ca^{2+} , Pb^{2+} , Cd^{2+} , Cu^{2+} , Co^{2+} , Zn^{2+} , Fe^{2+} , Mn^{2+} , Mg^{2+} , Ni^{2+} , Hg^{2+} , Na^+ , K^+ , Ag^+) from the nitrate, chloride or perchlorate salts were prepared with ultrapure water. **BHMH** (0.1 mM) was dissolved in DMF, which was then diluted by adding HEPES buffer (10 mM, pH 6.0) to 10 μM . The diluted solution DMF/ H_2O (1/1, v/v, 0.01M HEPES, pH = 6.0) was used for the measurement of UV-Vis spectra and fluorescence spectra. The excitation wavelength ($E_x = 420 \text{ nm}$) was used for fluorescence experiments and the slits including excitation and the emission all were set to 10 nm.

2.3. Synthesis

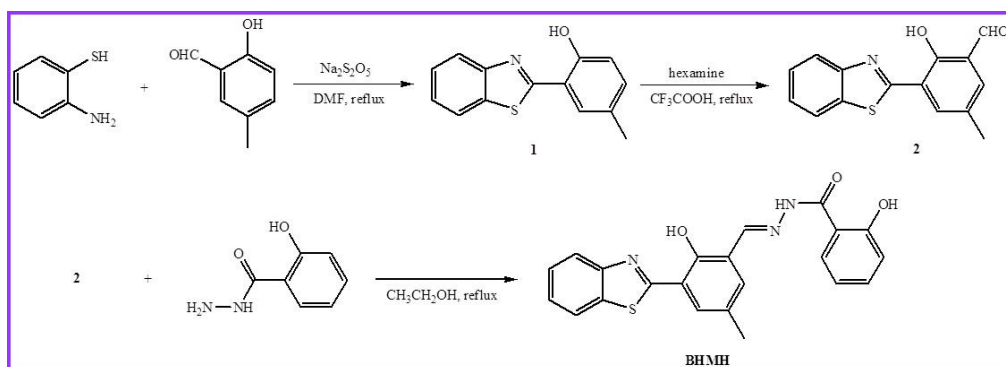
2.3.1 Synthesis of 2-(benzo[d]thiazol-2-yl)-4-methylphenol (**1**) and 3-(benzo[d]thiazol-2-yl)-2-hydroxy-5-methylbenzaldehyde (**2**)

Compounds **1** and **2** were synthesized according to reported methods [29], respectively.

2.3.2 Synthesis of (*E*)-3-(benzo[d]thiazol-2-yl)-2-hydroxy-5-methylbenzaldehyde salicyl acylhydrazone (**BHMH**)

Compound **2** (199 mg, 0.74 mmol) and 2-Hydroxybenzohydrazide (116 mg, 0.76 mmol) were dissolved in ethanol (30 mL), then the solution was refluxed until the completion of reaction (monitored by TLC). After cooling to room temperature, the solid was filtered and washed with ethanol (3 x 5 mL), then dried under vacuum to get yellow product **BHMH** (363 mg, yield 82%). m.p.: 278.4-280.2 °C. ^1H NMR (600 MHz, DMSO-d_6) (Fig. S1) δ (ppm): 13.25 (s, 1H), 12.25 (s, 1H), 11.68 (s, 1H), 8.75 (s, 1H), 8.21 (s, 1H), 8.18 (d, $J = 7.8 \text{ Hz}$, 1H), 8.09 (d, $J = 7.8 \text{ Hz}$, 1H), 7.91 (d, $J = 7.8 \text{ Hz}$, 1H), 7.61 (s, 1H), 7.56 (t, $J = 8.4 \text{ Hz}$, 1H), 7.48 (t, $J = 7.2 \text{ Hz}$, 2H), 7.02 (d, $J = 8.4 \text{ Hz}$, 1H), 7.00 (t, $J = 7.8 \text{ Hz}$, 1H), 2.41 (s, 3H). ^{13}C NMR (151 MHz, DMSO-d_6) (Fig. S2) δ

(ppm) 164.99, 163.95, 159.29, 154.54, 151.81, 148.99, 135.24, 134.57, 133.53, 131.08, 129.26, 129.21, 126.99, 125.66, 122.76, 122.53, 119.99, 119.87, 119.59, 117.78, 116.25, 20.41. HRMS (m/z) (TOF MS ES⁺) (Fig. S3): calcd for C₂₂H₁₇N₃O₃S: 404.1069 [M+H]⁺, found: 404.1061.



Scheme 2 Synthetic route of probe **BHMH**

3. Results and discussion

3.1. Sensing ability of **BHMH** to metal ions

Fluorescence selectivity of **BHMH** (Fig. 1a) in sensing different metal ions (Na⁺, K⁺, Ca²⁺, Fe²⁺, Ba²⁺, Mg²⁺, Mn²⁺, Ni²⁺, Cr³⁺, Cu²⁺, Fe³⁺, Co²⁺, Ag⁺, Cd²⁺, Zn²⁺, Hg²⁺, Al³⁺ and Pb²⁺) were firstly carried out in DMF/H₂O (1/1, v/v, 0.01M HEPES, pH = 6.0). The result showed that **BHMH** was highly selectivity to Al³⁺ and Zn²⁺ through significant fluorescent enhancement response accompanied with color change from yellow to deep green and light green, respectively. Consideration its specific fluorescent response to Al³⁺ and Zn²⁺, the UV-vis absorbance spectrum of **BHMH** were measured before and after addition of Al³⁺ and Zn²⁺ (Fig. 1b), respectively. Compared with **BHMH** itself, the addition of Al³⁺ and Zn²⁺ were all caused a significant change, respectively. The probe **BHMH** alone displayed two shoulder absorption peaks at 362 nm and 430 nm, which attributed to the π - π^* transition derived from the 2-(2'-hydroxyphenyl) benzothiazole chromophore during the ESIPT process of enol-keto automerization in the excited state [57, 58]. However, the addition of Al³⁺ and Zn²⁺ to the solution

of probe **BHMH** was all caused significant change which mainly reflected in the disappearance of absorption peak centered at 362 nm and obvious enhancement of that at 430 nm. Meanwhile, the solution color of probe **BHMH** was turned from colorless to pale green and green, respectively. This result displayed the existence of interaction between probe **BHMH** and Al^{3+} and Zn^{2+} .

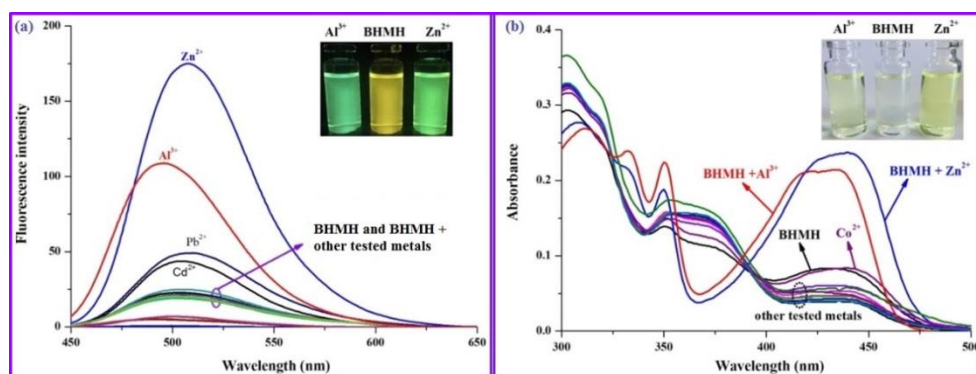


Fig. 1. Selectivity of **BHMH** to metal ions by spectra measurement of fluorescence (a) and UV-Vis absorbance (b).

In order to investigate the sensitivity of **BHMH** ($10\ \mu\text{M}$) to Al^{3+} and Zn^{2+} , the titration of fluorescence (**Fig. 2**) and UV-Vis absorbance (**Fig. 3**) were carried out in DMF/ H_2O (1/1, v/v, 0.01M HEPES, pH = 6.0), respectively. **BHMH** itself displayed weak fluorescent emission which might due to ESIPT process from hydroxyl group to its conjugated benzothiazole fluorophore. However, whatever the addition of metal ion was Al^{3+} or Zn^{2+} , fluorescence titration results of **BHMH** ($10\ \mu\text{M}$) were all showed a gradually enhancement in emission intensity attributed to the vanishment of ESIPT process after coordination of **BHMH** with $\text{Al}^{3+}/\text{Zn}^{2+}$. Moreover, based on the good relationship between **BHMH** ($10\ \mu\text{M}$) with Al^{3+} (0-5 μM) (**Fig. S4**) and Zn^{2+} (0-10 μM) (**Fig. S5**), the detection limit (LOD) of **BHMH** to Al^{3+} and Zn^{2+} which were calculated according to the reported equation ($\text{LOD} = 3\sigma/S$, where σ is the standard deviation of the blank solution and S is slope of calibration curve) [59-61] was $1.42 \times 10^{-7}\ \text{M}$ and $1.27 \times 10^{-7}\ \text{M}$, respectively. Moreover, the comparative analysis between **BHMH** and some previously reported sensors were summarized in Table 1.

Table 1. Comparison of different properties of **BHMH** with recently reported probes.

Ref.	Selectivity	Detection Medium	LOD	Binding Constants	Application
[38]	Al ³⁺	DMSO/H ₂ O (1:1)	3.7×10^{-9} M	1.16×10^4 M ⁻¹	Water sample
	Zn ²⁺		3.0×10^{-8} M	2.08×10^4 M ⁻¹	Cell imaging
[39]	Al ³⁺	CH ₃ OH	2.7×10^{-7} M	1.5×10^4 M ⁻¹	Water sample
	Zn ²⁺		4.0×10^{-8} M	6.4×10^4 M ⁻¹	Logic circuit
[40]	Al ³⁺	CH ₃ OH	2.97×10^{-9} M	1.27×10^4 M ⁻¹	Logic circuit
	Zn ²⁺		5.98×10^{-9} M	1.73×10^5 M ⁻¹	
[41]	Al ³⁺	DMSO	1.15×10^{-7} M	1.24×10^5 M ⁻¹	Logic circuit
	Zn ²⁺		5.27×10^{-7} M	9.70×10^4 M ⁻¹	
[42]	Al ³⁺	CH ₃ OH	NR	NR	Logic circuit
	Zn ²⁺	CH ₃ CN	NR	NR	
[43]	Al ³⁺	CH ₃ OH	6.72×10^{-9} M	4.61×10^4 M ⁻¹	Water sample
	Zn ²⁺	THF	7.02×10^{-8} M	2.06×10^4 M ⁻¹	Logic circuit
[44]	Al ³⁺	EtOH/H ₂ O (9:1)	1.77×10^{-7} M	5.40×10^9 M ⁻¹	Biological application
	Zn ²⁺		2.13×10^{-8} M	2.67×10^5 M ⁻¹	
	Cd ²⁺		5.76×10^{-8} M	1.37×10^3 M ⁻¹	
[45]	Al ³⁺	DMSO/H ₂ O (3:2)	1.20×10^{-6} M	2.5×10^3 M ⁻¹	Logic circuit
	Zn ²⁺		0.02×10^{-6} M	3.0×10^3 M ⁻¹	Cell imaging
[46]	Al ³⁺	DMSO	1.56×10^{-8} M	5.77×10^5 M ⁻¹	Cell imaging
	Zn ²⁺		1.62×10^{-8} M	3.87×10^5 M ⁻¹	
[47]	Al ³⁺	EtOH/H ₂ O (3:1)	3.18×10^{-6} M	1.61×10^4 M ⁻¹	Solid State
	Zn ²⁺		1.25×10^{-7} M	3.85×10^4 M ⁻¹	
[48]	Al ³⁺	DMSO/H ₂ O (9:1)	3.66×10^{-6} M	2.66×10^4 M ⁻¹	Cell imaging
	Zn ²⁺		1.01×10^{-6} M	1.08×10^5 M ⁻¹	
[49]	Al ³⁺	CH ₃ OH	2.13×10^{-6} M	6.65×10^3 M ⁻¹	Biological application
	Zn ²⁺		3.81×10^{-8} M	7.70×10^4 M ⁻¹	
[50]	Al ³⁺	CH ₃ OH/H ₂ O (9:1)	0.62×10^{-7} M	2.62×10^4 M ⁻¹	Water sample
	Zn ²⁺		1.67×10^{-7} M	1.92×10^4 M ⁻¹	Membrane sensing
[51]	Al ³⁺	CH ₃ OH/H ₂ O (7:3)	5.70×10^{-9} M	1.5×10^3 M ^{-1/2}	Water sample
	Zn ²⁺		1.09×10^{-6} M	5.0×10^5 M ⁻¹	
[52]	Al ³⁺	CH ₃ OH/H ₂ O (1:9)	8.04×10^{-7} M	1.66×10^4 M ⁻¹	Real sample
	Zn ²⁺		7.95×10^{-7} M	0.60×10^4 M ⁻¹	Cell imaging
[53]	Al ³⁺	EtOH/H ₂ O (95:5)	5.22×10^{-8} M	1.74×10^6 M ⁻¹	Water sample
	Zn ²⁺		7.88×10^{-8} M	6.45×10^2 M ^{-1/2}	Test paper
[54]	Al ³⁺	DMF/H ₂ O (96:4)	2.70×10^{-8} M	4.86×10^6 M ⁻¹	Cell imaging
	Zn ²⁺		3.30×10^{-8} M	3.10×10^7 M ⁻¹	
[55]	Al ³⁺	DMF/H ₂ O (9:1)	0.11×10^{-6} M	2.25×10^8 M ⁻²	NR
	Zn ²⁺		0.21×10^{-6} M	3.42×10^2 M ⁻¹	
This work	Al ³⁺	DMF/H ₂ O (1:1)	1.42×10^{-7} M	2.79×10^2 M ^{-1/2}	Water sample
	Zn ²⁺		1.27×10^{-7} M	3.19×10^4 M ⁻¹	Test paper

LOD: The limit of detection; NR: Not reported in the corresponding paper.

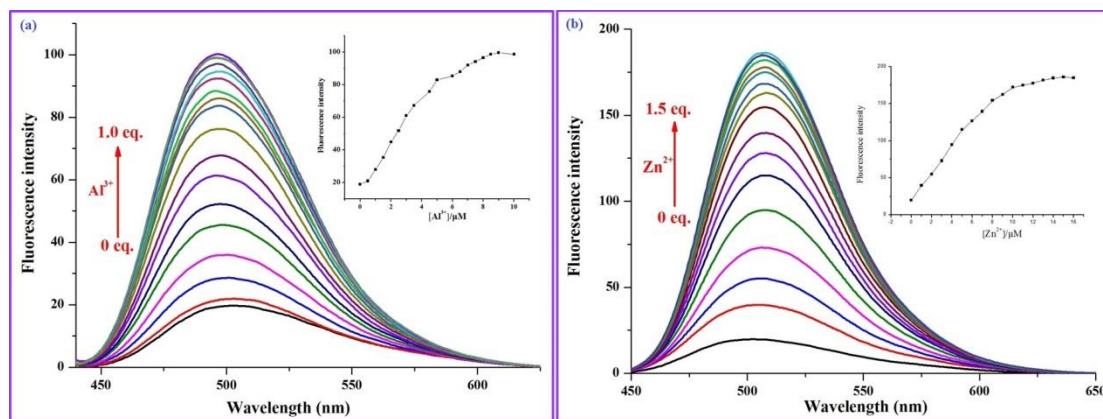


Fig. 2. (a) Fluorescence titration of **BHMH** to Al^{3+} . Inset: the ratio of fluorescence intensity of **BHMH** as a function of Al^{3+} concentration; (b) Fluorescence titration of **BHMH** to Zn^{2+} . Inset: the ratio of fluorescence intensity of **BHMH** as a function of Zn^{2+} concentration.

On the other hand, titration of UV-Vis absorbance for Al^{3+} (**Fig. 3a**) illustrated that the absorbance centered at 367 nm gradually disappeared while the shoulder absorbance peak at 435 nm was gradually increased with an obvious isobestic point at 388 nm, these findings indicated the complex formation of **BHMH** with Al^{3+} . In addition, the satisfied relationship was reached between the ratio of absorbance intensity (A_{435}/A_{367}) versus the Al^{3+} concentration (0-5 μM) (**Fig. S6**), indicated the achievement in ratiometric detection for Al^{3+} with the limit of detection (LOD) as 3.99×10^{-8} M which calculated according the reported method [29]. Similarly, upon the gradual addition of Zn^{2+} (0-10 μM), the absorbance at 366 nm decreased gradually and peak at 440 nm gradually enhanced accompanied with the formation of isobestic point at 392 nm at the same time (**Fig. 3b**), all of these supported the existence of interaction between **BHMH** and Zn^{2+} . The LOD for Zn^{2+} calculated as 3.32×10^{-8} M was satisfied based on the ratio of absorbance intensity (A_{440}/A_{366}) versus the Zn^{2+} concentration (0-5 μM) (**Fig. S7**), which also proved that **BHMH** was capable of used as ratiometric probe of Zn^{2+} .

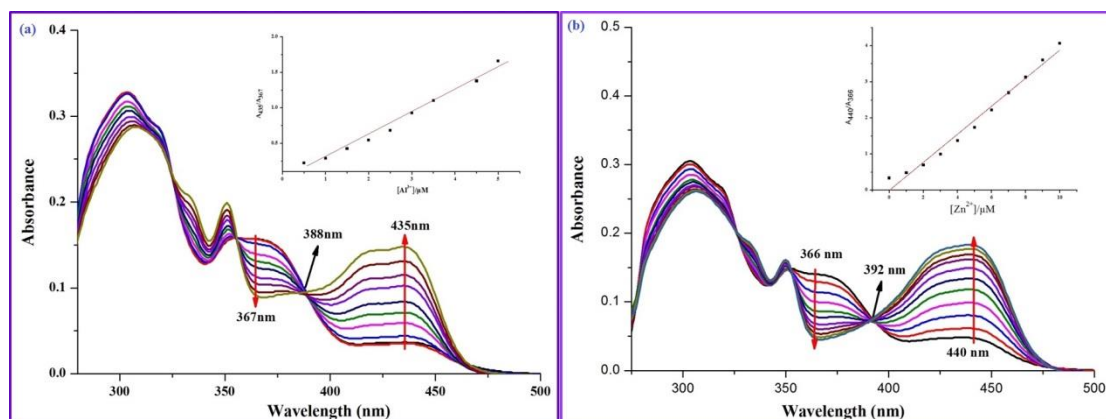


Fig. 3. (a) UV-Vis absorbance titration of **BHMH** to Al^{3+} . Inset: the ratio of absorbance (A_{435}/A_{367}) of **BHMH** as a function of Al^{3+} concentration; (b) Fluorescence titration of **BHMH** to Zn^{2+} . Inset: the ratio of absorbance (A_{440}/A_{366}) of **BHMH** as a function of Zn^{2+} concentration.

To further verify the anti-disturbance from other co-existence metal ions, the competition experiments (**Fig. 4**) for Al^{3+} and Zn^{2+} were carried out through measurement of fluorescence intensity (recorded $E_m=494$ nm for Al , and $E_m=508$ nm for Zn^{2+}) after adding other competition metal ions, respectively. The result showed that **BHMH** was sensitive enough to Al^{3+} and Zn^{2+} and could be used in the detection of Al^{3+} and Zn^{2+} in the existence of other tested ions.

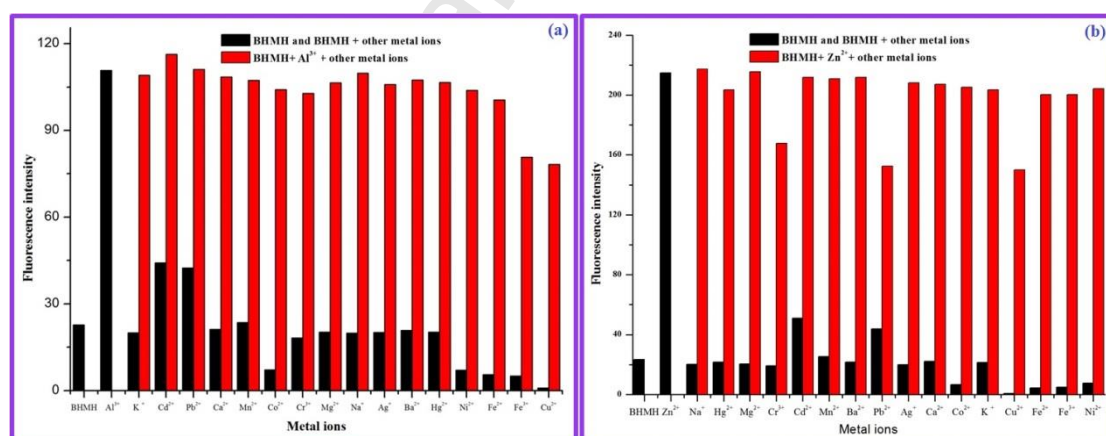


Fig. 4. Competition experiments of **BHMH** to Al^{3+} (a) and Zn^{2+} (b) in the presence of other metal ions.

Consideration the similarity response of **BHMH** to Al^{3+} and Zn^{2+} in the facet of color change either in daylight or UV-lamp, which was unfavorable in fast determination by naked-eye for one analyte containing Al^{3+} or Zn^{2+} . So, some efficient method should be found that which could be used to differentiate Al^{3+} from Zn^{2+} . EDTA, a valuable reagent which is usually used in

reversibility evaluation for one probe, was qualified to make a distinction between Al^{3+} and Zn^{2+} through adding it into the analyte solution. The phenomena was that the recognition process (Fluorescence spectrum and UV-Vis absorbance spectrum) (**Fig. 5**) for Zn^{2+} was reversible by alternate adding EDTA and Zn^{2+} , and which could be done at least 5 cycles assessed by fluorescence intensity (recorded at $E_m = 508 \text{ nm}$) (**Fig. 6a**) and color change (**Fig. 6b**). However, the above experimental method was out of validation for Al^{3+} that was the addition of EDTA could not recover the complex system of **BHMH**- Al^{3+} into **BHMH** itself (**Fig. S8**). Hence, this result supplied an efficient method in the fast estimation of Al^{3+} from Zn^{2+} .

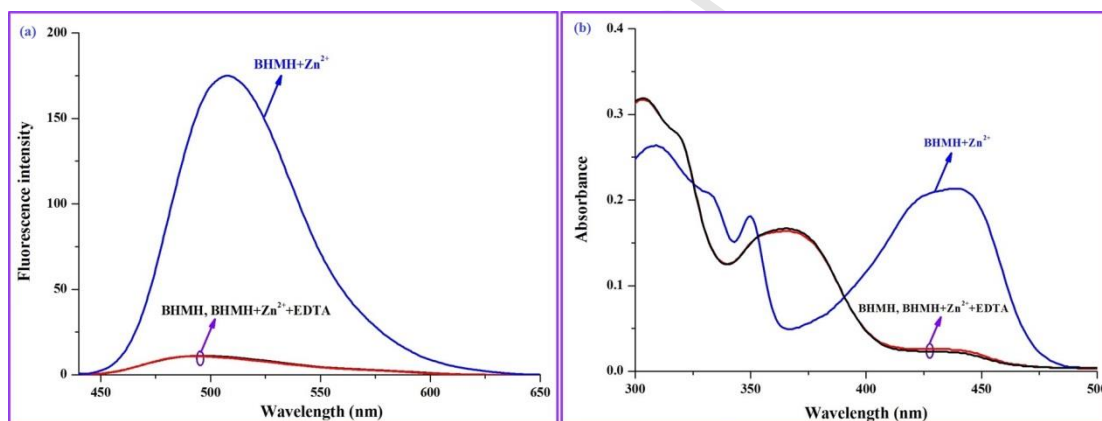


Fig. 5. Reversible experiments of **BHMH** to Zn^{2+} in fluorescence spectrum (a) and UV-Vis absorbance spectrum (b) by alternate adding EDTA and Zn^{2+} .

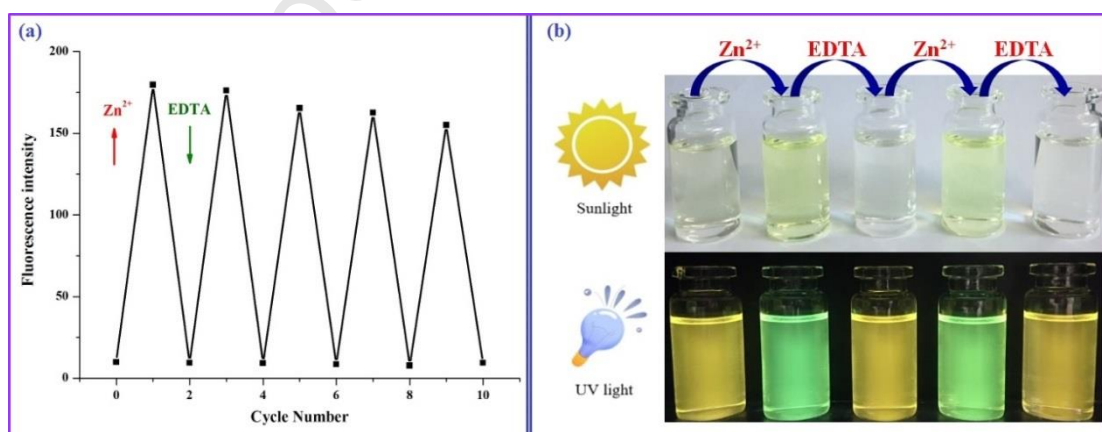


Fig. 6. Reversibility assessment of **BHMH** to Zn^{2+} by (a) fluorescence intensity ($E_m = 508 \text{ nm}$) and (b) color change under daylight (top) and UV-light (bottom).

3.2. Sensing mechanism of **BHMH** to Al^{3+} and Zn^{2+}

The Job's plot analysis (**Fig. 7**) was employed to determine the stoichiometry of **BHMH** with Al^{3+} and Zn^{2+} , respectively. The results showed that when the molar fraction was 0.3, the fluorescence intensity recorded at 494 nm for Al^{3+} reached maximum (**Fig. 7a**). While for Zn^{2+} recorded at 508 nm, the maximum molar fraction was 0.5 (**Fig. 7b**), all of these indicated that the binding ratio of **BHMH** was 2:1 for Al^{3+} while 1:1 for Zn^{2+} , respectively. According to the Benesi–Hildebrand plot [32, 62], the binding constants of Al^{3+} and Zn^{2+} with probe **BHMH** were $2.79 \times 10^2 \text{ M}^{-1/2}$ (**Fig. S9**) and $3.19 \times 10^4 \text{ M}^{-1}$ (**Fig. S10**), respectively.

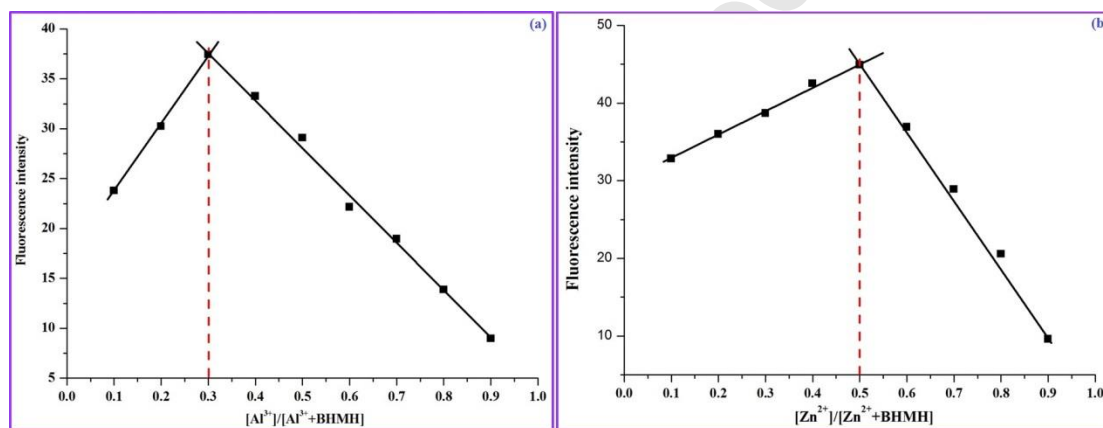


Fig. 7. Job plot for binding ratio between **BHMH** with Al^{3+} (a) and Zn^{2+} (b).

Furthermore, ESI-MS analyses were carried out to investigate the coordination detail of **BHMH** with Al^{3+} and Zn^{2+} in DMF solution (**Fig. 8**), respectively. Peaks at m/z 831.1631 and 404.1054 were designated to $[\text{2(BHMH} - \text{H}^+) + \text{Al}^{3+}]^+$ (Calcd: 831.1640) which was a supplementary proof for the 2:1 binding ratio concluded by job plot, and $[\text{BHMH} + \text{H}^+]^+$ (Calcd: 404.1061) illustrated in the spectra of **BHMH** + Al^{3+} (**Fig. 8a**). As for the spectra of **BHMH** + Zn^{2+} (**Fig. 8b**), peaks at m/z 404.1056, 539.0719 and 612.1244 were respectively attributed to $[\text{BHMH} + \text{H}^+]^+$ (Calcd: 404.1061), $[\text{BHMH} - \text{H}^+ + \text{Zn}^{2+} + \text{DMF}]^+$ (Calcd: 539.0731) and $[\text{BHMH} - \text{H}^+ + \text{Zn}^{2+} + 2\text{DMF}]^+$ (Calcd: 612.1259) which also to some extent indicated the 1:1 complex formation between **BHMH** and Zn^{2+} . These results further confirmed the formation of

stable complexes between probe **BHMH** and $\text{Al}^{3+}/\text{Zn}^{2+}$, respectively.

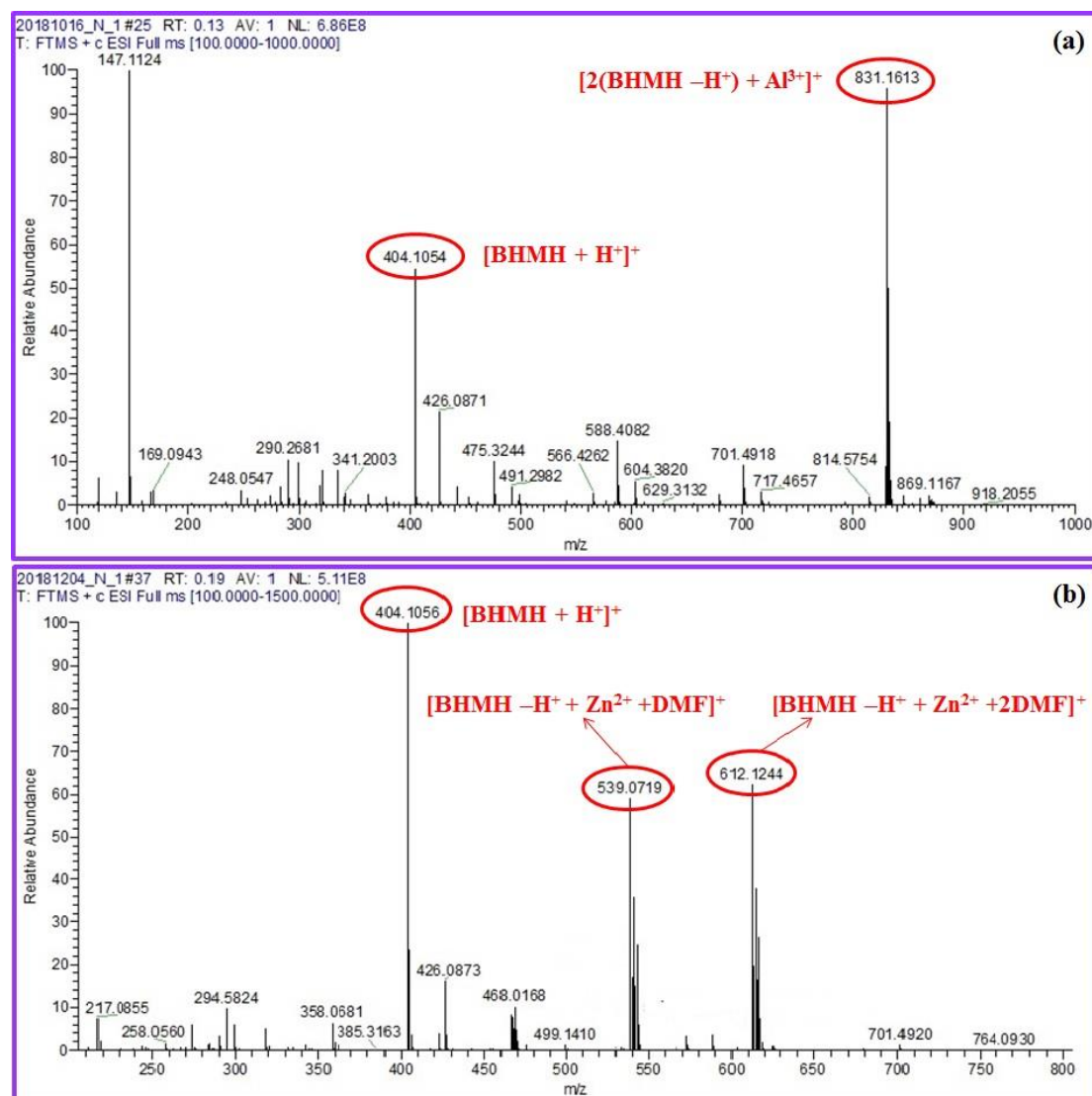


Fig. 8. ESI-MS spectrum of **BHMH** (10 μM) upon addition of Al^{3+} (a) and Zn^{2+} (b) in DMF.

To precisely master the binding detail of **BHMH** with $\text{Al}^{3+}/\text{Zn}^{2+}$, FT-IR spectra were firstly measured in the absence and presence of $\text{Al}^{3+}/\text{Zn}^{2+}$ (**Fig. S11**), respectively. The result showed that the FT-IR spectrum of **BHMH** itself had its characteristic peaks including the stretching frequency of amide group (-NH), phenolic hydroxyl group (-OH), carbonyl group (C=O) and imide group (C=N), which were located at 3444 cm^{-1} , 3260 cm^{-1} , 1624 cm^{-1} and 1539 cm^{-1} , respectively. As for the FT-IR spectrum of **BHMH- Al^{3+}** (**Fig. S11a**), the stretching bands of phenolic hydroxyl group (-OH) of **BHMH** was disappeared, indicated the deprotonation of phenolic hydroxyl group

of **BHMH** during the binding process with Al^{3+} . Furthermore, the stretching bands intensity of the carbonyl group (C=O) and imide group (C=N) were all significant decreased, indicated the interaction between the carbonyl group (C=O) and Al^{3+} . While the FT-IR spectra of **BHMH-Zn²⁺** (**Fig. S11b**), the characteristic stretching bands of amide group (-NH) and phenolic hydroxyl group (-OH) were obviously shifted to 3161cm^{-1} and 3056cm^{-1} , indicating the interaction of **BHMH** with Zn^{2+} through the phenolic hydroxyl group (-OH) and carbonyl group (C=O).

^1H NMR titrations were measured to further investigate the interaction between **BHMH** and $\text{Al}^{3+}/\text{Zn}^{2+}$ through compared with **BHMH** itself. The proton signals located at 13.26 ppm, 12.26 ppm and 11.68 ppm were designated to the phenolic hydroxyl (H_g) and (H_k), and the amide (H_b) groups of **BHMH** in the (*E*)-configuration (**Fig. 9**) which was the dominated configuration in Schiff-base molecular, respectively. Upon gradual addition of Al^{3+} , the signal of H_g was almost disappeared and its integral area was obviously decreased according to the integral area ratio (H_g : H_k : H_j) (**Fig. S12**), indicating the deprotonation on hydroxyl group during the combination of **BHMH** with Al^{3+} , while the intensity of the other two signals (H_k and H_j) were gradual weakened and their corresponding signals in (*Z*)-configuration were gradual appeared at 10.34 ppm (H_k) and 9.24 ppm (H_j), respectively. This result indicated the configuration changed from (*Z*)-configuration to (*E*)-configuration after coordination with Al^{3+} which coordinated with oxygen atom came from the deprotonation of phenolic hydroxyl (H_g). As for the titration of Zn^{2+} (**Fig. 10**), the proton signal of the phenolic hydroxyl (H_g) was decreased and its integral area was also reduced upon the gradual addition of Zn^{2+} (**Fig. S13**), and the proton signal of the phenolic hydroxyl (H_k) and amide (H_j) were all weakened gradually, indicating the deprotonation of the phenolic hydroxyl (H_g) on probe **BHMH** upon the coordination with Zn^{2+} .

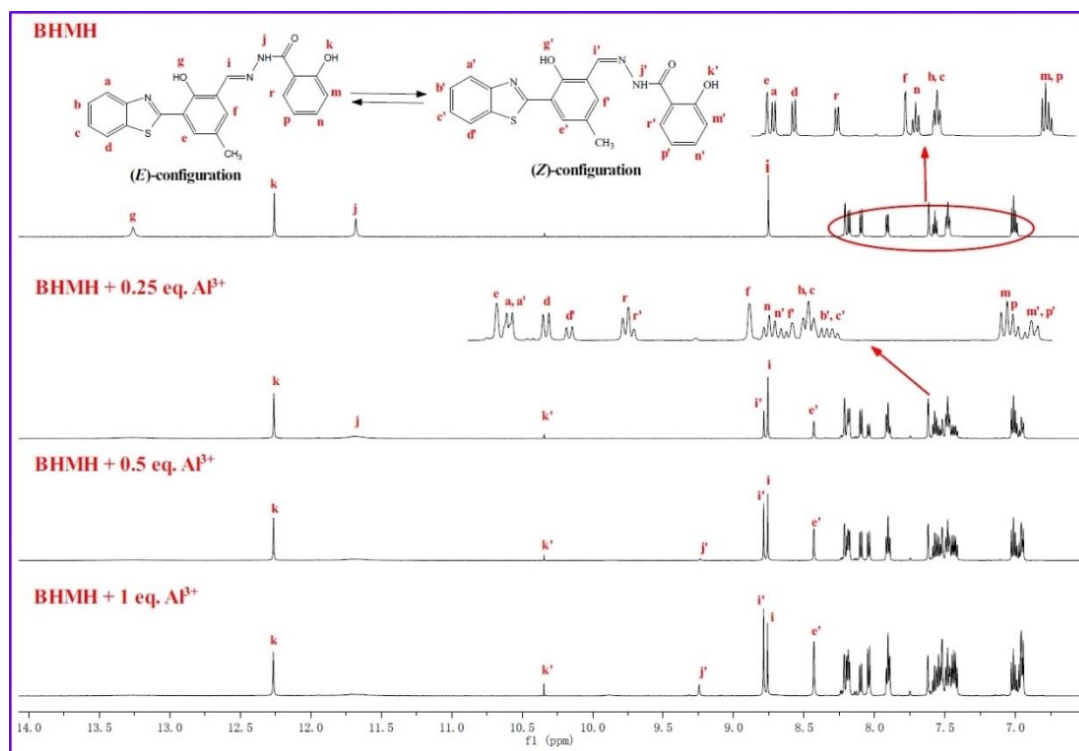


Fig. 9. ^1H NMR spectra of **BHMH** with Al^{3+} in DMSO-d_6 .

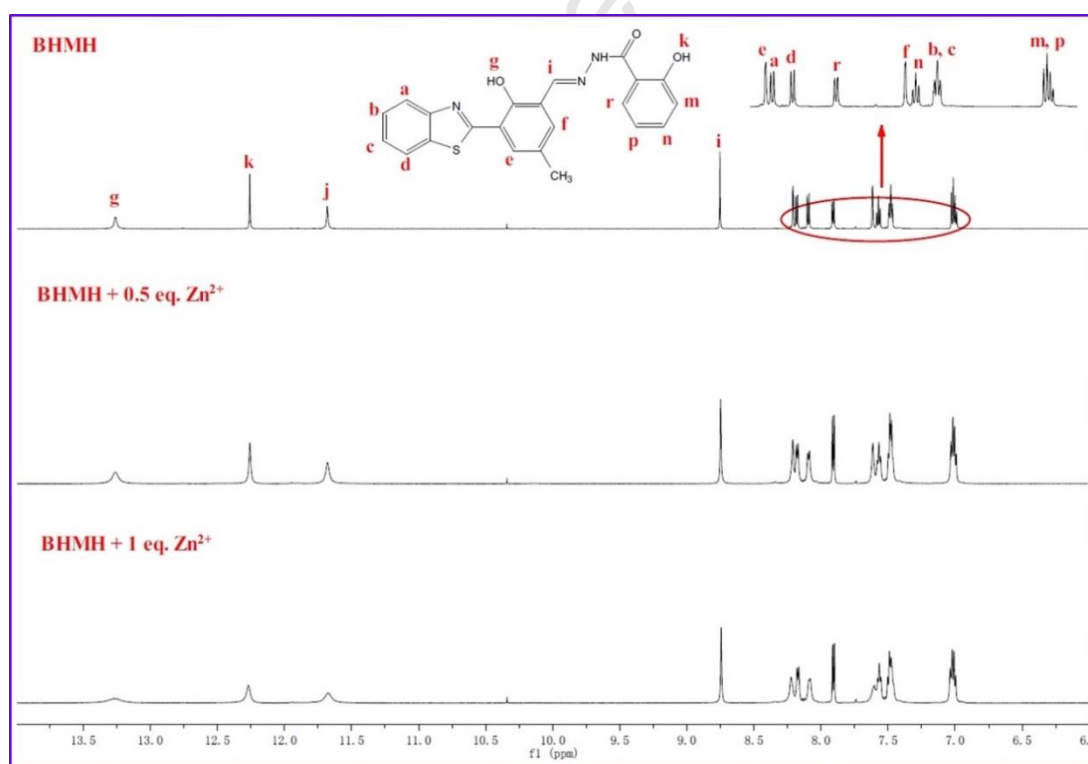
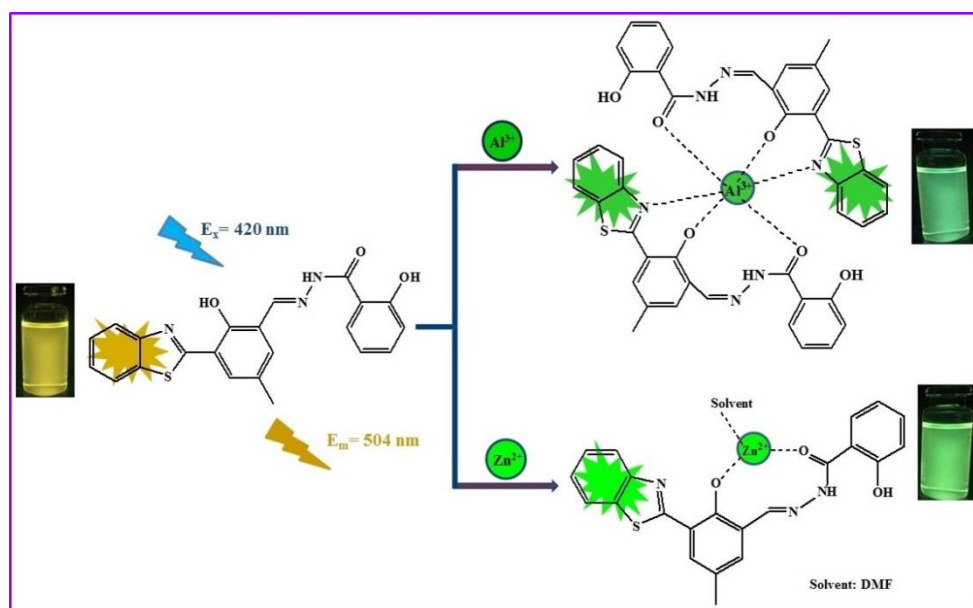


Fig. 10. ^1H NMR spectra of **BHMH** with Zn^{2+} in DMSO-d_6 .

According to the above launched experimental results containing job' plot, FT-IR, HRMS, and ^1H NMR titration, the probable sensing mechanism of both **BHMH**- Al^{3+} and **BHMH**- Zn^{2+} was illustrated in **Scheme 3**.



Scheme 3 Plausible sensing mechanism of **BHMH** to Al^{3+} and Zn^{2+} .

3.3. pH effect on **BHMH** with Al^{3+} and Zn^{2+}

In order to estimate the effect caused by pH change on **BHMH** for the detection of Al^{3+} and Zn^{2+} , the fluorescence spectra of **BHMH** upon addition of Al^{3+} and Zn^{2+} were measured in different pH condition (**Fig. 11**), respectively. The result indicated that the idea pH ranges for **BHMH** in the detection of Al^{3+} (**Fig. 11a**) and Zn^{2+} (**Fig. 11b**) were 4-7 and 5-7, respectively.

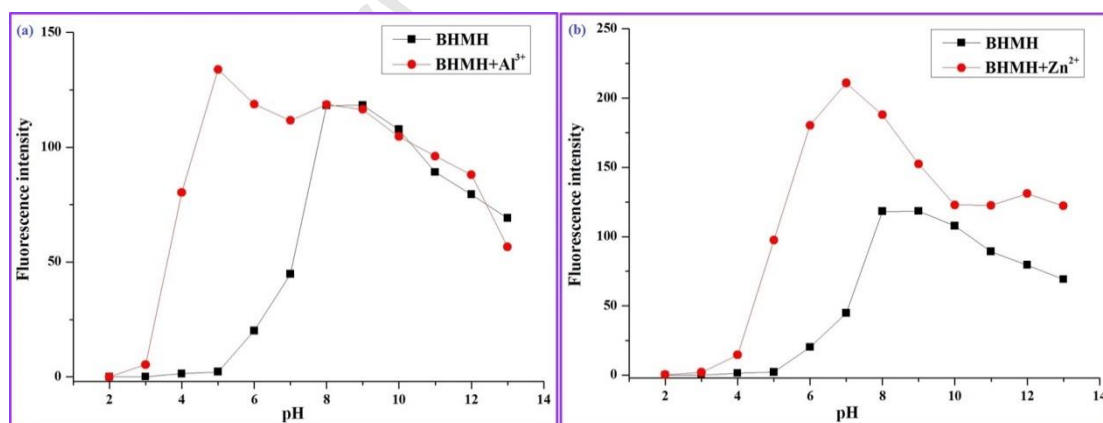


Fig. 11. The fluorescent response of **BHMH** (10 μM) in the absence and presence of Al^{3+} (a) and Zn^{2+} (b) in $\text{DMF}/\text{H}_2\text{O}$ (1/1, v/v) at different pH medium, respectively.

3.4. Application of **BHMH**

3.4.1 Detection Al^{3+} and Zn^{2+} in water samples

Probe **BHMH** for the determination of Al^{3+} and Zn^{2+} were firstly carried out in real water

sample to verify its practical application. These water samples were collected from campus of our university and Songhua River in Heilongjiang Province, and Al^{3+} and Zn^{2+} at different levels (1-10 μM) were spiked by those water samples, respectively. The fluorescence responses of Probe **BHMH** were recorded for sensing Al^{3+} at 494 nm and Zn^{2+} at 508 nm (**Fig. 12**), respectively. The results showed that with the increase of concentration of either Al^{3+} (**Fig. 12a**) or Zn^{2+} (**Fig. 12b**) in tested samples (including ultrapure water, tap water and Songhua water), the fluorescence intensity were all increased gradually, and the good linearity was found between fluorescence intensity and $\text{Al}^{3+}/\text{Zn}^{2+}$ over the concentration range of 1-10 μM (**Fig. S14-19**), respectively. The desirable recovery and relative standard deviations (R.S.D) values (Table S1 and S2) indicated that Probe **BHMH** could be applied in quantitative analysis in real water sample for the detection of Al^{3+} and Zn^{2+} .

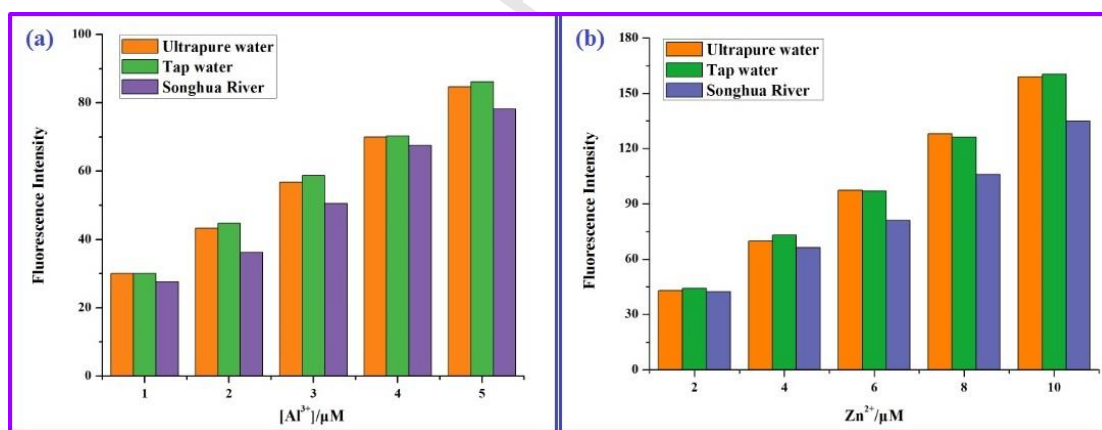


Fig. 12. Fluorescent detection of **BHMH** (10 μM) in “ultrapure water”, “tap water”, and “Songhua River” upon addition of different concentration of (a) Al^{3+} ($E_m = 494$ nm) and (b) Zn^{2+} ($E_m = 508$ nm), respectively.

3.4.2 Detection Al^{3+} and Zn^{2+} on test paper

Fast and portable detection for one analyte was one important factor to evaluate a probe's application property. Hence, the test paper experiments for sensing Al^{3+} and Zn^{2+} were investigated through fluorescence color change (**Fig. 13**), respectively. Test papers were obtained by which was immersed in **BHMH** solution containing different concentrations of Al^{3+} (0, 1, 2, 3,

4 and 5 μM) and Zn^{2+} (0, 2, 4, 6, 8 and 10 μM), respectively. After dried in air, accompanied with the increasing concentration of Al^{3+} (**Fig. 13**, top) and Zn^{2+} (**Fig. 13**, bottom) under 365 nm ultraviolet light, the color of the test papers were gradually changed from ivory to light blue and light green, respectively. Moreover, the differentiate Al^{3+} from Zn^{2+} on test paper was further investigated by adding EDTA, and the procedure was recorded as Video S1. The first step was that the dried test papers which had been immersed in **BHMH** (50 μM) solution containing the same concentrations of Al^{3+} (50 μM) and Zn^{2+} (50 μM) were put on the watch glass, respectively. The second step was that the same quality EDTA (50 μL) was added onto the test papers. The result showed that the color of test paper (containing Zn^{2+}) turned from blackish green into the bright orange similar as the color of the solid of **BHMH** under the under 365 nm ultraviolet light, indicated the regeneration of **BHMH**. However, the test paper (containing Al^{3+}) almost showed no color change after the addition of EDTA, which was similar to the result of differentiation experiments of Al^{3+} from Zn^{2+} in **BHM** solution by adding EDTA. The above results indicated that the probe **BHMH** can detect Al^{3+} or Zn^{2+} conveniently in the actual sample through the test paper.

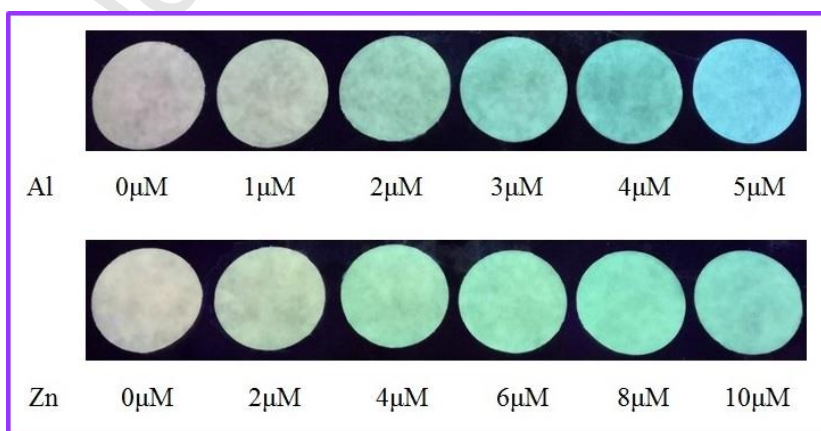


Fig. 13. The image of probe **BHMB** on test strips with different concentrations of Al^{3+} (top) and Zn^{2+} (bottom) under 365 nm UV light, respectively.

4. Conclusion

In conclusion, a simple ESIPT-based dual-functional probe **BHMH** was designed and synthesized which displayed fluorescence turn-on and absorbance ratiometric detection for Al^{3+} and Zn^{2+} . The 1:1 stoichiometry concerning the complex of **BHMH** - Al^{3+} and **BHMH** - Zn^{2+} were confirmed by Job's plot, respectively. Especially, **BHMH** was achieved in making a distinction between Zn^{2+} and Al^{3+} by adding the EDTA reagent through either fluorescence or absorbance response. Moreover, probe **BHMH** was successfully achieved in the detection Al^{3+} and Zn^{2+} in real water samples as well as fast and portable detection by test strips.

Declaration of competing interest

The authors declare no competing financial interest

Acknowledgements

This work was supported by the Postdoctoral Scientific Research Developmental Fund of Heilongjiang Province (No. LBH-Q14023), and Students' Innovation and Entrepreneurship Training Program of Northeast Agricultural University (No. 201910224325).

References

- [1] R.A. Yokel, The toxicology of aluminum in the brain: a review, *Neurotoxicology* 21 (2000) 813-828.
- [2] A. Mirza, A. King, C. Troakes, C. Exley. Aluminium in brain tissue in familial Alzheimer's disease, *J.Trace Elem. Med. Bio.* 40 (2017) 30-36.
- [3] C. Exley, The coordination chemistry of aluminium in neurodegenerative disease, *Coordin.*

- Chem. Rev. 256 (2012) 2142-2146.
- [4] I. Ivanovski, A. Ivanovski, D. Nikolić, P. Ivanovski, Aluminium in brain tissue in autism, J. Trace Elem. Med. Bio. 51 (2019) 138–140.
- [5] M. Mold, D. Umar, A. King, C. Exley, Aluminium in brain tissue in autism, J. Trace Elem. Med. Bio. 46 (2018) 76-82.
- [6] P.F. Good, C.W. Olanow, D.P. Perl, Neuromelanin-containing neurons of the substantia nigra accumulate iron and aluminum in Parkinson's disease: a LAMMA study, Brain Res. 593 (1992) 343–346.
- [7] Z.C. Xu, J. Yoon, D.R. Spring, Fluorescent chemosensors for Zn^{2+} , Chem. Soc. Rev. 39 (2010) 1996-2006.
- [8] E.L. Que, D.W. Domaille, J. Chang Christopher, Metals in Neurobiology: Probing Their Chemistry and Biology with Molecular Imaging, Chem. Rev. 108 (2008) 1517-1549.
- [9] A. Takeda, H. Tamano, Insight into zinc signaling from dietary zinc deficiency, Brain. Res. Rev. 62 (2009) 33-44.
- [10] B.B. McAllister, R.H. Dyck, Zinc transporter 3 (ZnT_3) and vesicular zinc in central nervous system function, Neurosci. Biobehav. Rev. 80 (2017) 329-350.
- [11] C. Migliorini, E. Porciatti, M. Luczkowski, D. Valensin, Structural characterization of Cu^{2+} , Ni^{2+} and Zn^{2+} binding sites of model peptides associated with neurodegenerative diseases, Coord. Chem. Rev. 256 (2012) 352-368.
- [12] D. Wu, L. Chen, W. Lee, G. Ko, J. Yin, J. Yoon. Recent progress in the development of organic dye based near-infrared fluorescence probes for metal ions, Coord. Chem. Rev. 354 (2018) 74-97.

- [13] J.A. Kaczmarek, J.A. Mitchell, M.A. Spence, V. Vongsouthi, C.J. Jackson. Structural and evolutionary approaches to the design and optimization of fluorescence-based small molecule biosensors, *Curr. Opin. Struc. Biol.* 57 (2019) 31-38.
- [14] B.M. Luby, D.M. Charron, C.M. MacLaughlin, G. Zheng, Activatable fluorescence: From small molecule to nanoparticle. *Adv. Drug Deliver. Rev.* 113 (2017) 97–121.
- [15] H. Lu, C. Yu, S. Xu, A dual reference ion-imprinted ratiometric fluorescence probe for simultaneous detection of silver (I) and lead (II), *Sensors Actuators B Chem.* 288 (2019) 691-698.
- [16] J. Zhang, X. Ji, J. Zhou, Z. Chen, X. Dong, W. Zhao, Pyridinium substituted BODIPY as NIR fluorescent probe for simultaneous sensing of hydrogen sulphide/glutathione and cysteine/homocysteine, *Sensors Actuators B Chem.* 257 (2018) 1076-1082.
- [17] F. Chen, D. Han, Y. Gao, H. Liu, S. Wang, F. Zhou, K. Li, S. Zhang, W. Shao, Y. He, A turn-on fluorescent probe for simultaneous sensing of cysteine/homocysteine and hydrogen sulfide and its bioimaging applications, *Talanta* 187 (2018) 19-26.
- [18] J. Huang, Y. Chen, J. Qi, X. Zhou, L. Niu, Z. Yan, J. Wang, G. Zhao, A dual-selective fluorescent probe for discriminating glutathione and homocysteine simultaneously, *Spectrochim. Acta A Mol. Biomol. Spectrosc.* 201 (2018) 105-111.
- [19] J. Xu, N. Liu, C. Hao, Q. Han, Y. Duan, J. Wu, A novel fluorescence “on-off-on” peptide-based chemosensor for simultaneous detection of Cu^{2+} , Ag^+ and S^{2-} , *Sensors Actuators B Chem.* 280 (2019) 129-137.
- [20] Y. Gao, C. Zhang, S. Peng, H. Chen, A fluorescent and colorimetric probe enables simultaneous differential detection of Hg^{2+} and Cu^{2+} by two different mechanisms, *Sensors*

- Actuators B Chem. 238 (2017) 455-461.
- [21] A.I. Said, N.I. Georgiev, V.B. Bojinov, Synthesis of a single 1,8-naphthalimide fluorophore as a molecular logic lab for simultaneously detecting of Fe^{3+} , Hg^{2+} and Cu^{2+} , Spectrochim. Acta A Mol. Biomol. Spectrosc. 196 (2018) 76-82.
- [22] S.Y. Lee, K.H. Bok, T.G. Jo, S.Y. Kim, C. Kim, A simple Schiff-base fluorescence probe for the simultaneous detection of Ga^{3+} and Zn^{2+} , Inorg. Chim. Acta 461 (2017) 127-135.
- [23] T. Yu, G. Yin, T. Niu, P. Yin, H. Li, Y. Zhang, H. Chen, Y. Zeng, S. Yao, A novel colorimetric and fluorescent probe for simultaneous detection of $\text{SO}_3^{2-}/\text{HSO}_3^-$ and HSO_4^- by different emission channels and its bioimaging in living cells, Talanta 176 (2018) 1-7.
- [24] L. Zhai, Z. Shi, Y. Tu, S. Pu, A dual emission fluorescent probe enables simultaneous detection and discrimination of Cys/Hcy and GSH and its application in cell imaging, Dyes Pigments, 165 (2019) 164-171.
- [25] X. Ren, H. Tian, L. Yang, L. He, Y. Geng, X. Liu, X. Song, Fluorescent probe for simultaneous discrimination of Cys/Hcy and GSH in pure aqueous media with a fast response under a single-wavelength excitation, Sensors Actuators B Chem. 273 (2018) 1170-1178.
- [26] Y. Zhang, Q. Tu, L. Chen, N. Li, L. Yang, X. Zhang, M.S. Yuan, J. Wang, A fluorescein-based AND-logic FPSi probe for the simultaneous detection of Hg^{2+} and F^- , Talanta 202 (2019) 323-328.
- [27] H. Niu, B. Ni, K. Chen, X. Yang, W. Cao, Y. Ye, Y. Zhao, A long-wavelength-emitting fluorescent probe for simultaneous discrimination of $\text{H}_2\text{S}/\text{Cys}/\text{GSH}$ and its bio-imaging applications, Talanta 196 (2019) 145-152.
- [28] S. Chen, Y. Kuang, P. Zhang, Y. Huang, A. Wen, X. Zeng, R. Feng, H. Nie, X. Jiang, Y. Long,

- A dual-functional spectroscopic probe for simultaneous monitoring Cu^{2+} and Hg^{2+} ions by two different sensing nature based on novel fluorescent gold nanoclusters, *Sensors Actuators B Chem.* 253 (2017) 283-291.
- [29] S. Zeng, S.J. Li, X.J. Sun, T.T. Liu, Z.Y. Xing, A dual-functional chemosensor for fluorescent on-off and ratiometric detection of Cu^{2+} and Hg^{2+} and its application in cell imaging, *Dyes Pigments* (2019), <https://doi.org/10.1016/j.dyepig.2019.107642>.
- [30] L. Yan, M. Yang, X. Leng, M. Zhang, Y. Long, B. Yang, A new dual-function fluorescent probe of Fe^{3+} for bioimaging and probe- Fe^{3+} complex for selective detection of CN^- , *Tetrahedron* 72 (2016) 4361-4367.
- [31] L. Zong, C. Wang, Y. Song, Y. Xie, P. Zhang, Q. Peng, Q. Li, Z. Li, A dual-function probe based on naphthalene diimide for fluorescent recognition of Hg^{2+} and colorimetric detection of Cu^{2+} , *Sensors Actuators B Chem.* 252 (2017) 1105-1111.
- [32] N.N. Li, Y.Q. Ma, X.J. Sun, M.Q. Li, S. Zeng, Z.Y. Xing, J.L. Li, A dual-function probe based on naphthalene for fluorescent turn-on recognition of Cu^{2+} and colorimetric detection of Fe^{3+} in neat H_2O , *Spectrochim. Acta A Mol. Biomol. Spectrosc.* 210 (2019) 266-274.
- [33] F. Ye, X.M. Liang, K.X. Xu, X.X. Pang, Q. Chai, Y. Fu, A novel dithiourea-appended naphthalimide “on-off” fluorescent probe for detecting Hg^{2+} and Ag^+ and its application in cell imaging, *Talanta* 200 (2019) 494-502.
- [34] Y. Wang, Y. F. Song, L. Zhang, G. G. Dai, R. F. Kang, W. N. Wu, Z. H. Xu, Y. C. Fan, L. Y. Bian, A pyrazole-containing hydrazone for fluorescent imaging of Al^{3+} in lysosomes and its resultant Al^{3+} complex as a sensor for F^- , *Talanta* 203 (2019) 178-185.
- [35] Y.P. Wu, F.U. Rahman, M.Z. Bhatti, S.B. Yu, B. Yang, H. Wang, Z.T. Li, D.W. Zhang,

- Acylylhydrazone as a novel “Off–On–Off” fluorescence probe for the sequential detection of Al^{3+} and F^- , *New J. Chem.* 42 (2018) 14978-14985.
- [36] P. Ding, J. Wang, J. Cheng, Y. Zhao, Y. Ye, Three N-stabilized rhodamine-based fluorescent probes for Al^{3+} via Al^{3+} -promoted hydrolysis of Schiff bases, *New J. Chem.* 39 (2015) 342-348.
- [37] S. Erdemir, M. Yuksekogul, S. Karakurt, O. Kocuyigit, Dual-channel fluorescent probe based on bisphenol A-rhodamine for Zn^{2+} and Hg^{2+} through different signaling mechanisms and its bioimaging studies, *Sensors Actuators B Chem.* 241 (2017) 230-238.
- [38] Y. Li, Q. Niu, T. Wei, T. Li, Novel thiophene-based colorimetric and fluorescent turn-on sensor for highly sensitive and selective simultaneous detection of Al^{3+} and Zn^{2+} in water and food samples and its application in bioimaging, *Anal. Chim. Acta* 1049 (2019) 196-212.
- [39] W. Gao, Y. Zhang, H. Li, S. Pu, A multi-controllable selective fluorescent turn-on chemosensor for Al^{3+} and Zn^{2+} based on a new diarylethene with a 3-(4-methylphenyl)-1H-pyrazol-5-amine Schiff base group, *Tetrahedron* 74 (2018) 6299-6309.
- [40] Y. Liang, L. Diao, R. Wang, N. Wang, S. Pu, A bifunctional probe for Al^{3+} and Zn^{2+} based on diarylethene with an ethylimidazo[2,1-b]thiazole-6-hydrazide unit, *Tetrahedron Lett.* 60 (2019) 106–112.
- [41] R. Lu, S. Cui, S. Li, S. Pu, A highly sensitive and selective fluorescent sensor for Al^{3+} and Zn^{2+} based on diarylethene with an aminouracil unit, *Tetrahedron* 73 (2017) 915-922.
- [42] L. Ma, G. Liu, S. Pu, C. Zheng, C. Fan, Solvent-dependent selective fluorescence sensor for Zn^{2+} and Al^{3+} based on a new diarylethene with a salicylal schiff base group, *Tetrahedron* 73 (2017) 1691-1697.

- [43] Z. Wang, S. Cui, S. Qiu, S. Pu, A dual-functional fluorescent sensor based on diarylethene for Zn^{2+} and Al^{3+} in different solvents, *J. Photochem. Photobiol. A Chem.* 376 (2019) 185-195.
- [44] J. Sun, B. Ye, G. Xia, H. Wang, A multi-responsive squaraine-based “turn on” fluorescent chemosensor for highly sensitive detection of Al^{3+} , Zn^{2+} and Cd^{2+} in aqueous media and its biological application, *Sensors Actuators B Chem.* 249 (2017) 386-394.
- [45] A. K. Bhanja, C. Patra, S. Mondal, S. Mishra, K. D. Saha, C. Sinha, Macrocyclic aza-crown chromogenic reagent to Al^{3+} and fluorescence sensor for Zn^{2+} and Al^{3+} along with live cell application and logic operation, *Sensors Actuators B Chem.* 252 (2017) 257-267.
- [46] Y. Wang, W.W. Wang, W.Z. Xue, W.N. Wu, X.L. Zhao, Z.Q. Xu, Y.C. Fan, Z.H. Xu, A simple hydrazone as a fluorescent turn-on multianalyte (Al^{3+} , Mg^{2+} , Zn^{2+}) sensor with different emission color in DMSO and resultant Al^{3+} complex as a turn-off sensor for F^- in aqueous solution, *J. Lumin.* 212 (2019) 191-199.
- [47] B. Pang, C. Li, Z. Yang, A novel chromone and rhodamine derivative as fluorescent probe for the detection of Zn(II) and Al(III) based on two different mechanisms, *Spectrochim. Acta A Mol. Biomol. Spectrosc.* 204 (2018) 641-647.
- [48] Z. Liao, Y. Liu, S.F. Han, D. Wang, J.Q. Zheng, X.J. Zheng, L.P. Jin, A novel acylhydrazone-based derivative as dual-mode chemosensor for Al^{3+} , Zn^{2+} and Fe^{3+} and its applications in cell imaging, *Sensors Actuators B Chem.* 244 (2017) 914-921.
- [49] W. Li, X. Tian, B. Huang, H. Li, X. Zhao, S. Gao, J. Zheng, X. Zhang, H. Zhou, Yupeng Tian, J. Wu, Triphenylamine-based Schiff bases as the High sensitive Al^{3+} or Zn^{2+} fluorescence turn-on probe: Mechanism and application in vitro and in vivo, *Biosens. Bioelectron.* 77 (2016) 530-536.

- [50] L. K. Kumawat, M. Asif, V. K. Gupta, Dual ion selective fluorescence sensor with potential applications in sample monitoring and membrane sensing, *Sensors Actuators B Chem.* 241 (2017) 1090-1098.
- [51] N. Behera, V. Manivannan, A Probe for Multi Detection of Al^{3+} , Zn^{2+} and Cd^{2+} Ions via Turn-On Fluorescence Responses, *J. Photochem. Photobiol. A Chem.* 353 (2018) 77-85.
- [52] B. K. Kundu, P. Mandal, B. G. Mukhopadhyay, R. Tiwari, D. Nayak, R. Ganguly, S. Mukhopadhyay, Substituent dependent sensing behavior of Schiff base chemosensors in detecting Zn^{2+} and Al^{3+} ions: Drug sample analysis and living cell imaging, *Sensors Actuators B Chem.* 282 (2019) 347-358.
- [53] S. Erdemir, O. Kocuyigit, Dual recognition of Zn^{2+} and Al^{3+} ions by a novel probe containing two fluorophore through different signaling mechanisms, *Sensors Actuators B Chem.* 273 (2018) 56-61.
- [54] H. Zhang, T. Sun, Q. Ruan, J.L. Zhao, L. Mu, X. Zeng, Z. Jin, S. Su, Q. Luo, Y. Yan, C. Redshaw, A multifunctional tripodal fluorescent probe for the recognition of Cr^{3+} , Al^{3+} , Zn^{2+} and F^- with controllable ESIPT processes, *Dyes Pigments* 162 (2019) 257-265.
- [55] G.R. Suman, S.G. Bubbly, S.B. Gudennavar, V. Gayathri, Benzimidazole and benzothiazole conjugated Schiff base as fluorescent sensors for Al^{3+} and Zn^{2+} , *J. Photochem. Photobiol. A Chem.* (2019), <https://doi.org/10.1016/j.jphotochem.2019.111947>.
- [56] S. Zeng, S.J. Li, X.J. Sun, M.Q. Li, Z.Y. Xing, Jin-Long Li, A benzothiazole-based chemosensor for significant fluorescent turn-on and ratiometric detection of Al^{3+} and its application in cell imaging. *Inorg. Chim. Acta* 486 (2019) 654-662.
- [57] B. Gu, L. Huang, W. Su, X. Duan, H. Li, S. Yao, A benzothiazole-based fluorescent probe

- for distinguishing and bioimaging of Hg^{2+} and Cu^{2+} , *Anal. Chim. Acta* 954 (2017) 97-104.
- [58] K.I. Hong, W. H. Choi, W.D. Jang, Hydroxythiophene-bearing benzothiazole: Selective and sensitive detection of periodate and its application as security ink, *Dyes Pigments* 162 (2019) 984-989.
- [59] L. Kang, Z.Y. Xing, X.Y. Ma, Y.T. Liu, Y. Zhang, A highly selective colorimetric and fluorescent turn-on chemosensor for Al^{3+} based on naphthalimide derivative, *Spectrochim. Acta A Mol. Biomol. Spectrosc.* 167 (2016) 59-65.
- [60] L. Kang, Y.T.Liu, N.N. Li, Q.X. Dang, Z.Y. Xing, J.L. Li, Y. Zhang, A schiff-base receptor based naphthalimide derivative: Highly selective and colorimetric fluorescentturn-on sensor for Al^{3+} , *J. Lumin.* 186 (2017) 48-52.
- [61] Y. Fu, X.X. Pang, Z. Q. Wang, Q. Chai, F. Ye, A highly sensitive and selective fluorescent probe for determination of Cu (II) and application in live cell imaging, *Spectrochim. Acta A Mol. Biomol. Spectrosc.* 208 (2019) 198-205.
- [62] S. Zeng, S.J. Li, X.J. Sun, M.Q. Li, Y.Q. Ma, Z.Y. Xing, J.L. Li, A naphthalene-quinoline based chemosensor for fluorescent “turn-on” and absorbance-ratiometric detection of Al^{3+} and its application in cells imaging, *Spectrochim. Acta A Mol. Biomol. Spectrosc.* 205 (2018) 276-286.

CRediT author statement

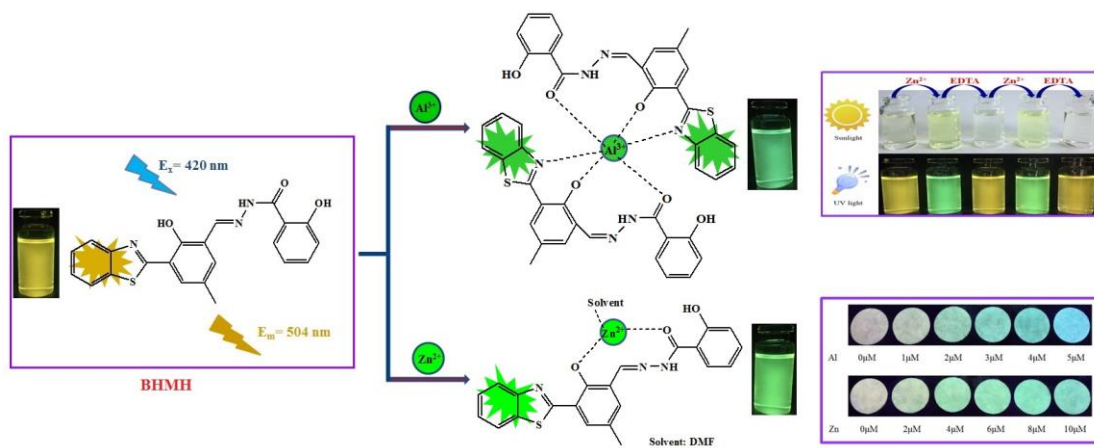
Liu Ting-Ting: Data curation, Writing-original draft; **Xu Jiao:** Formal analysis; **Liu Cheng-guo:** Investigation; **Zeng Shuang:** Validation; **Xing Zhi-Yong:** Conceptualization, Methodology, Writing-review & editing; **Sun Xue-Jiao:** Visualization; **Li Jin-Long:** Supervision.

Declaration of interests

The authors declare that they have no known competing financial interests or personal relationships that could have appeared to influence the work reported in this paper.

The authors declare the following financial interests/personal relationships which may be considered as potential competing interests:

Graphical abstract



Highlights

- Chemosensor **BHMH** with benzothiazole fluorophore was synthesized and characterized.
- **BHMH** exhibits highly selective to Zn^{2+} and Al^{3+} with significant fluorescence turn-on and color change.
- Limit of detection (LOD) for Zn^{2+} and Al^{3+} were all reached the level of 10^{-8} M.
- **BHMH** was successfully applied in the detection of Zn^{2+} and Al^{3+} in test paper.